Available online at www.scholarsresearchlibrary.com

Scholars Research Library

Archives of Physics Research, 2010: 1 (1) 75-87
(http://scholarsresearchlibrary.com/archive.html)

Rietveld Refinement,Microstructure and Electrical Properties of $PbTiO_3$ Ceramic Materials

Niranjan Sahu[1*], Manoranjan Kar[2]and S. Panigrahi[1]

[1]*Department of Physics, National Institute of Technology, Rourkela, Orissa, India*
[2]*Department of Physics, Indian Institute of Technology, Patna, India*

Abstract

$PbTiO_3$ compound was prepared by following the solid state route. X-ray diffraction (XRD) pattern was recorded at room temperature. Sample is found to be in single phase form. All the observed peaks could be indexed to P4mm space group with tetragonal symmetry. The XRD pattern has been analyzed by employing Rietveld method. The unit cell parameters are found to be a=b=3.8987(0.0008)Å and c=4.1380(0.0009)Å. The axial ratio c/a and unit cell volume is found to be 1.0614 and 62.896(0.023)Å^3 respectively. Bond lengths and bond angles have been calculated using the cell parameters. The average axial and in plane bond lengths are found to be 1.8865Å and 2.0026Å respectively. SEM-EDS indicate that the material is uniform and the composition at different places was found to be identical. The average crystallite size was found to be 202.832nm by using Scherrer's equation. The variation of dielectric constant and loss tangent with temperature and frequency of the sample was also investigated and the observed behavior is explained qualitatively.

PACS: 61.05,-cp;77.80.-e;77.80.Bh;77.84.Dy;

Keywords: Rietveld method; $PbTiO_3$; XRD; SEM-EDS; Tetragonal; Ferroelectric;

Introduction

The perovskites structure has been one of most versatile structure [1, 2] for tailoring the properties of materials. Lead titanate ($PbTiO_3$, PT), has drawn considerable interest in fundamental research due to its rich physical properties. This material shows high Curie temperature and possesses high spontaneous polarization. It is a ferroelectric material that presents a Curie temperature of 490^{0}C and displays pyroelectric and piezoelectric properties [1-8]. This material is being considered for applications in different kinds of devices, such as storage information, piezoelectric actuators, infrared sensors and ultrasonic transducers in medical and solar applications [9-11]. Recently lots of effort has been given to prepare the bulk as well as thin film of $PbTiO_3$. However, a large tetragonality (c/a=1.063) of tetragonal phase PT resulting in a high stress within the lattice leads to a frangibility and brings difficulty to prepare corresponding ceramics [12]. Recently, the isomorphic substitution of lead with lanthanum gives rise to a decrease in the tetragonality, and the material with a formula of $Pb_{0.7}La_{0.3}TiO_3$ (PLT30) has a pseudo cubic perovskite structure [13-15]. However, according to our knowledge, the detailed structural analysis for $PbTiO_3$ prepared at different temperatures and method is lagging to short out the synthesis of stable $PbTiO_3$. We have prepared PT by solid state route to study its crystal structure. The detailed crystal structure has been studied by analyzing the XRD pattern recorded at room temperature. The XRD pattern has been analyzed by employing Rietveld method and the help of Fullprof software [16]. Ananta and Thomas [17] found Pb volatility in PMN-PT could be minimized by careful sintering up to 1000ºC. What is clear is that the losses depend on particle size, processing conditions and chemical stability. The degree of Pb incorporation into the Presintered crystal structure affects the volatility enormously [18]. Many groups report that Pb-loss may be minimized by sintering compacted powders in a surrounding Pb-based powder or a PbO vapor atmosphere [19, 20] although this may lead to a Pb gradient in the final sintered product. It is clear from these investigations that it is commonly believed that a fine grain size in PT is essential for high density and little or no micro cracking. It is particularly interesting to discover that the ferroelectric perovskite $PbTiO_3$ behaves more closely in the expected manner. It undergoes a first order transition at 493ºC from cubic perovskite to a tetragonal ferroelectric phase isomorphic with tetragonal $BaTiO_3$ [21-23], but no additional transitions are as yet definitely established. To our knowledge this kind of finding was still to develop and one could observe how dielectric constant increases drastically at transition temperature (T_c=493ºC). Finally, the variation of dielectric constant and loss tangent with temperature and frequency of the sample was also investigated and the observed behavior is explained qualitatively.

Materials and Methods

Experimentation

$PbTiO_3$ compound was prepared by following solid state route. Stoichiometric ratio of $Pb(NO_3)_2$ and TiO_2 with 99.9% purity were weighed by using a high precision electronic balance with 5 digit accuracy (Avon, Gr 202). The above materials were mixed thoroughly with the help of agate mortar and pestle. The grinding was carried out under acetone till the acetone evaporates from the mortar. The mixture was presintered at 600^0C for 36hrs with intermediate grindings. The sintering in pellet form was carried out at 1000^0C for over 40hrs with intermediate grindings and repelletizing. All the above sintering processes were carried out in air. The detailed flow diagram for the preparation of $PbTiO_3$ is given in fig.1. The scanning electron micrograph was recorded using SEM (Jeol T-330 Scanning Electron Microscope).The compositional analysis was carried out by SEM EDS. XRD pattern at room temperature for the sample was recorded by using Bruker D 8 Advance XRD machine. The CuK_α radiation was used as X-Ray source. The machine was operated at 35KV and 30mA. The data was collected with step size of 0.01^0 and time constant of 1second.After polishing the PT ceramic sample, silver paste was applied on the flat surface of the pellets for electrical characterization. Relative dielectric constants (ε_r) and dielectric loss (tanδ) was measured as a function temperature and frequency using computer interfaced Solartron SI 1260 (Model) IMPEDANCE/GAIN-PHASE ANALYZER.

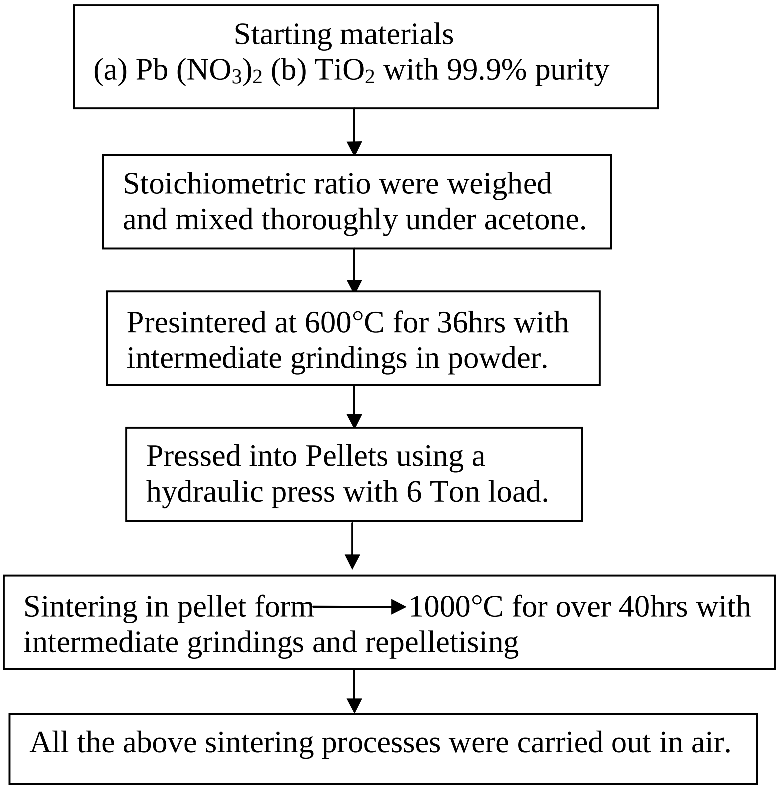

Fig. 1. Flow diagram for the processing of PT ceramics with powders prepared by solid state route

Results and Discussion

XRD patterns were recorded at room temperature using a BRUKER D-8 ADVANCE XRD machine by employing CuK_{α} radiation. The XRD patterns recorded for $PbTiO_3$ compound is shown in Fig. 2. One can see that the sample is essentially in single phase form within the instrumental error. All the observed peaks could be indexed to *P4mm* space group with tetragonal symmetry. The XRD pattern was refined by Rietveld method and by using the fullprof program [16]. The refined XRD pattern is shown in Fig. 3. The experimental points are given as plus (+) and theoretical data are shown as solid line. Difference between theoretical and experimental data is shown as bottom line. The vertical lines represent the Bragg's allowed peaks. The XRD peaks were generated by using *P4mm* space group, i.e. in tetragonal symmetry. The pseudo-voight function was chosen for the profile shape refinement because it is used to resolve strain and size contribution to peak broadening moreover it is the linear combination of Lorentzian and Gaussian function. The refinement was carried out by allowing the variation of different parameters such as, cell parameters, scale factors, position parameters, and isotropic thermal parameters. The position of the Pb, Ti and O atoms are given in table – 1. Two oxygen positions were taken for the refinement. The occupancy was taken as fixed as it is a lighter atom; hence it is not very sensitive to the XRD. It is difficult to refine the oxygen occupancy from XRD data. The scaning electron micrograph and EDS measurement are shown in fig: 4 which indicate that the material is uniform and the compositions at different places are found to be identical.

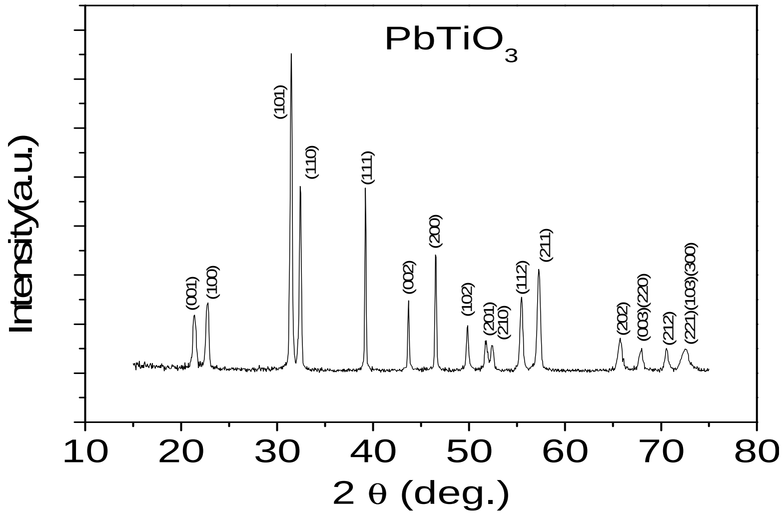

Fig.2. The XRD pattern of $PbTiO_3$. Observed peaks are indexed to *P4mm* space group

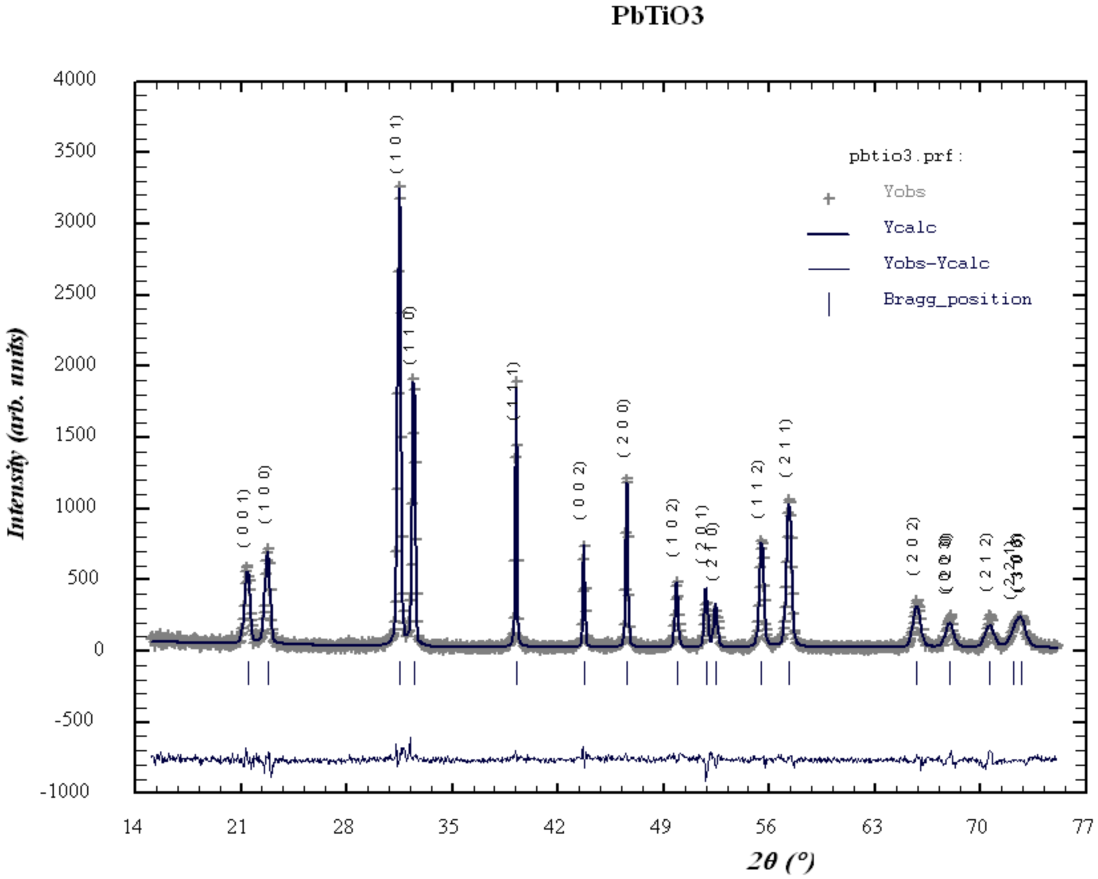

Fig. 3. XRD pattern for $PbTiO_3$ with refined data obtained by Rietveld method. The experimental points are given as plus (+) and theoretical data are shown as solid line. Difference between theoretical and experimental data is shown as bottom line. The vertical lines represent the Bragg's allowed peaks.

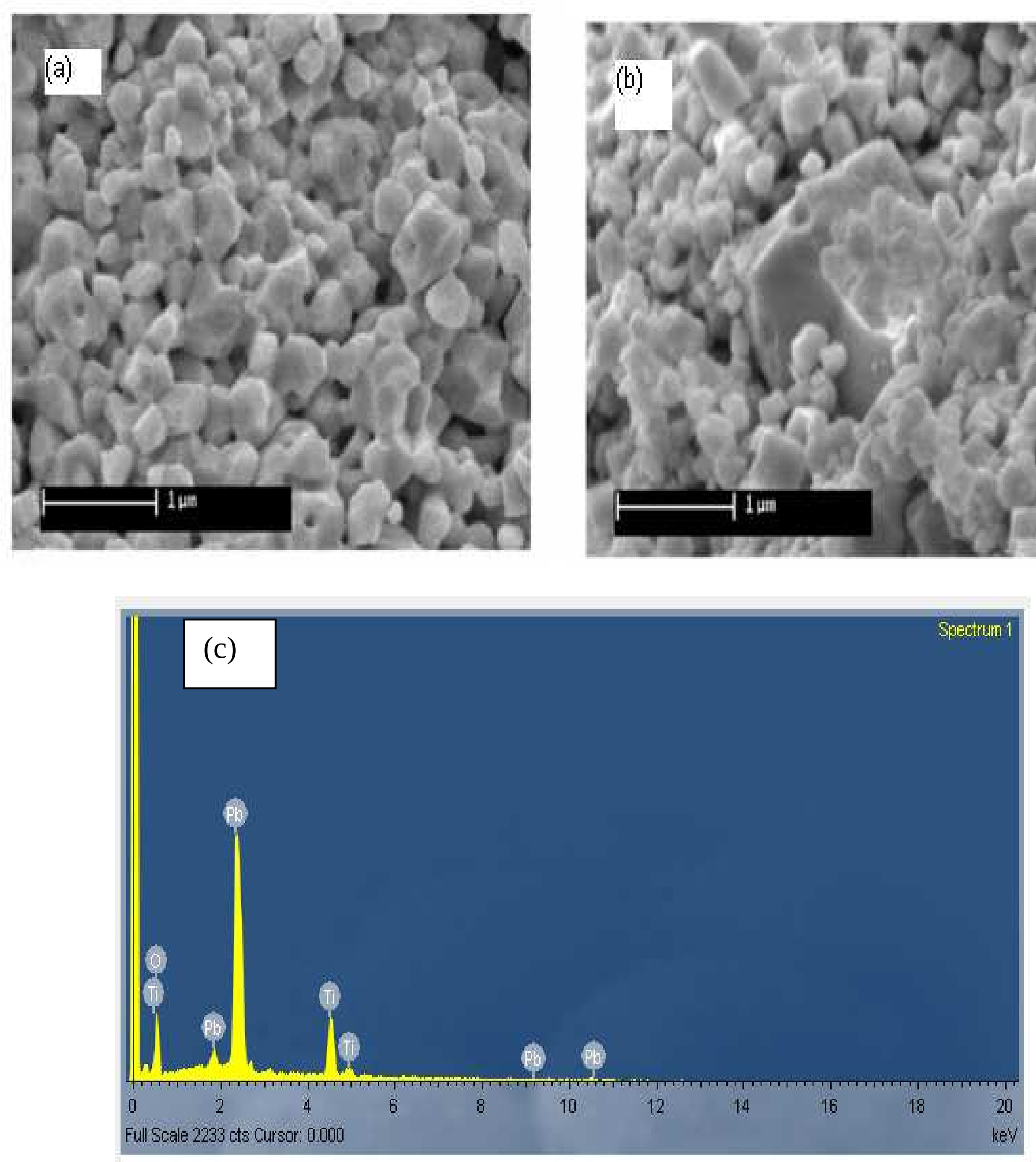

Fig.4. (a) The SEM of $PbTiO_3$ powder sintered at 1000°C for over 40 hrs and (b) The SEM of $PbTiO_3$ powder Presintered at 600°C for over 36 hrs(c) EDS measurement of PT powder annealed at 1000°C for over 40hrs

SEM micrographs of the fracture surfaces of compacts annealed at 600°C and 1000°C are shown in Figs. 4a and b, respectively. Fig. 4a shows that the sample has developed a relatively uniform microstructure with a grain size of 200–400 nm. Some residual porosity is visible and the fracture appears to have been intergranular. Sintering at1000°C leads to a superficially similar microstructure except that some abnormal grain growth occurs. For example, a large grain is visible in Fig. 4b (around 1.5–2.5 µm in diameter) surrounded by smaller particles. Overall, at 1000°C, the particle size distribution is much broader. There are areas of the fracture surface with a regular arrangement of small grains, whereas in other areas grains as large as 5.6 µm have grown. It is likely that the growth of large grains locally increases internal stresses and leads to cracking in the bulk ceramic on cooling [24]. Fig.4c shows that the sample has developed a relatively uniform microstructure with a grain size of 210nm[26]. Some residual porosity is visible and the fracture appears to have been intergranular and the composition at different places was found to be identical.

Table 1: Position parameters of Pb, Ti, O1 and O2

Atom	X	Y	Z
Pb	0.00000	0.00000	0.00000
Ti	0.50000	0.50000	0.53000
O1	0.50000	0.50000	0.07410
O2	0.50000	0.00000	0.64090

The refined cell parameters are found to be a = b = 3.8987(0.0008) Å and c = 4.1380 (0.0009) Å. These values are found to be comparable to those of in ref. 12. The unit cell volume is found to be 62.896(0.023) Å. The goodness of fit parameters are found to be R_p=3.70, R_{wp}= 4.20, R_{exp}=3.91, R_{Bragg}= 5.63, R_f = 3.20 and χ^2 = 1.32. The axial ratio c/a is found to be 1.0614 which is less then that of earlier reported value 1.063 [12]. The low axial value shows that the material is more compact and structure is more stable. Hence we could prepare the material with less axial ratio by following the solid state route.

The bond lengths and bond angles were calculated from the refined data with the help of Powdercell programme. The average axial and in plane bond lengths are found to be 1.8865Å and 2.0026Å respectively. All the bond lengths are listed in table 2. These values are found to be comparable with those reported in the literature. All the calculated bond angles are listed in table 3 and these are comparable with that of earlier literature values. The structure of the compound is shown in fig. 5. This structure has been drawn using the refined parameters.

Table 2: Bond Length using the parameters obtained from Rietveld analysis

No	Atom1	Atom2	Distance	Quant
1	Pb	TI	3.5228	4
2	TI	O1	1.8865	1
3	TI	O2	2.0026	4
4	TI	Pb	3.3738	4
5	O2	Pb	2.4511	8

Table 3: Bond angles calculated using the parameters obtained from Rietveld analysis

Atom1	Atom2	Atom3	Angle	Quant
Pb	TI	O1	51.4957	3
Pb	TI	O2	66.6733	6
Pb	TI	Pb	67.1950	4
Pb	TI	O2	132.9454	6
Pb	TI	Pb	102.9922	2
Pb	TI	PB	73.7068	2
Pb	TI	Pb	111.0323	8
Pb	TI	Pb	176.6986	1
O1	TI	O2	103.2468	2
O1	TI	O2	103.2477	2
O1	TI	Pb	51.4965	1
O1	TI	Pb	125.2020	1
O1	TI	Pb	125.2026	3
O2	TI	O2	86.9897	3
O2	TI	Pb	132.9445	2
O2	TI	O2	153.5056	2
O2	TI	Pb	46.0113	6
O2	TI	Pb	46.0119	2
O2	TI	Pb	115.4878	6
TI	O2	Pb	97.9855	6
Pb	TI	O2	66.6742	2
Pb	TI	Pb	73.7063	2
Pb	TI	PB	176.6984	3
O2	TI	O2	86.9893	1
O2	TI	Pb	115.4871	2
TI	O2	Pb	97.9861	2
Pb	TI	Pb	70.5908	2
Pb	TI	Pb	109.5952	2
TI	Pb	O2	36.0032	8
Pb	TI	Pb	70.5904	2
Pb	O2	Pb	105.3639	4
O2	Pb	O2	68.4369	3
O2	Pb	O2	68.4363	1

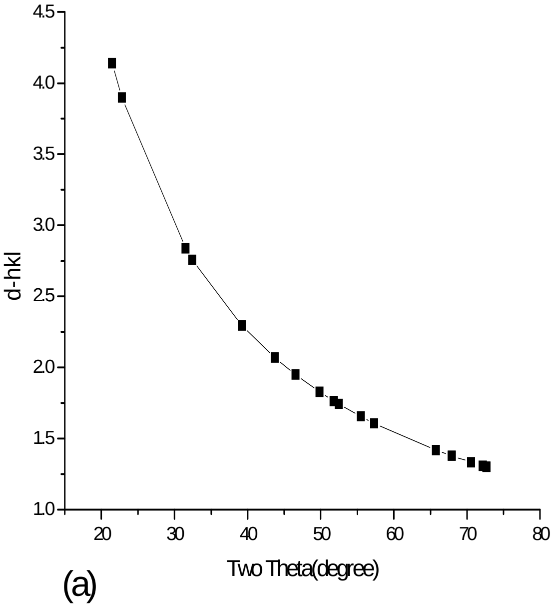

(a)

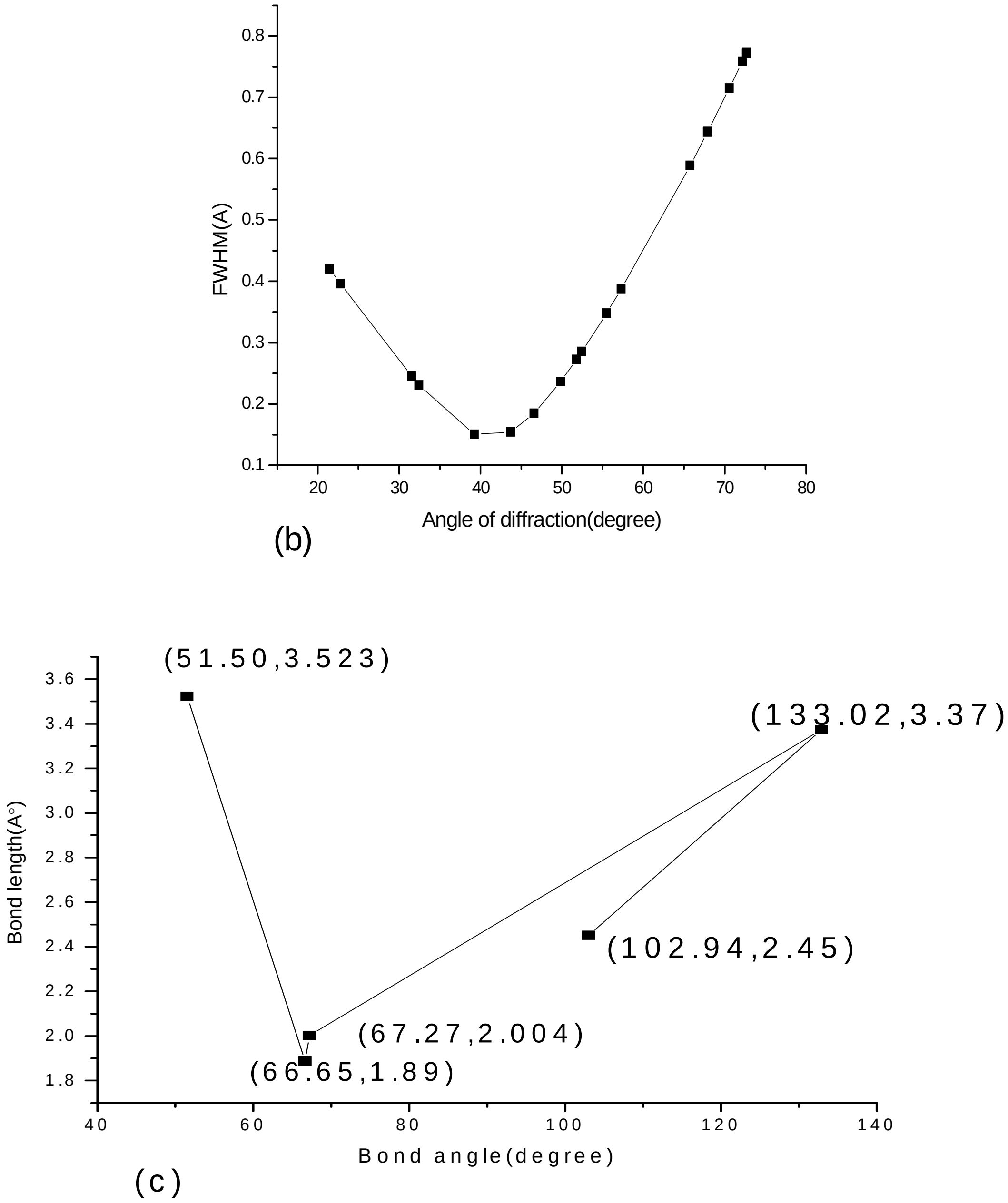

Fig: 5(a) Shows d-spacing and angle of diffraction (b) Shows Full width half maximum (β) and angle of diffraction (c) Shows the bond lengths and bond angles obtained from Rietveld analysis

From fig5. (a) indicates that the value of d-spacing decreases with increase of glancing angle. (b) shows that full width half maximum(FWHM) (β) starts decreases from the glancing angle ∠19 to ∠40 then suddenly increases with increase of angle of diffraction.(c) shows that at the bond length 3.523 the bond angle is ∠51.50.when the bond angle increases from ∠51.50 to ∠66.65

then one can observe its bond length decreases half of its original value. Again from bond angle ∠66.65 to ∠133.02 its bond lengths slightly increase and then decreases with the angles. From this study one can conclude that minimum bond angles are having maximum bond lengths which indicate that structure is more stable and compact. So one can prepare a stable and compact structure for better alignment of atoms.

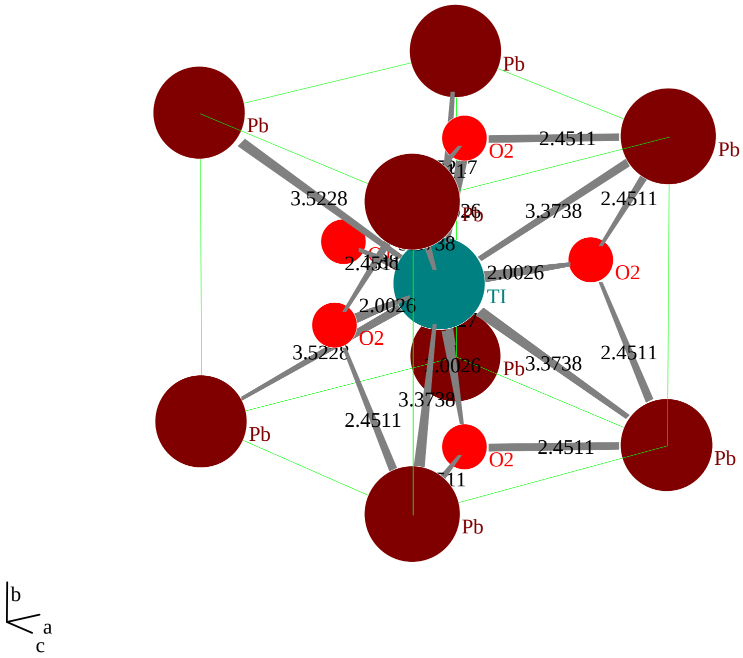

Fig.6. Structure of $PbTiO_3$ obtained from the Rietveld analysis parameters

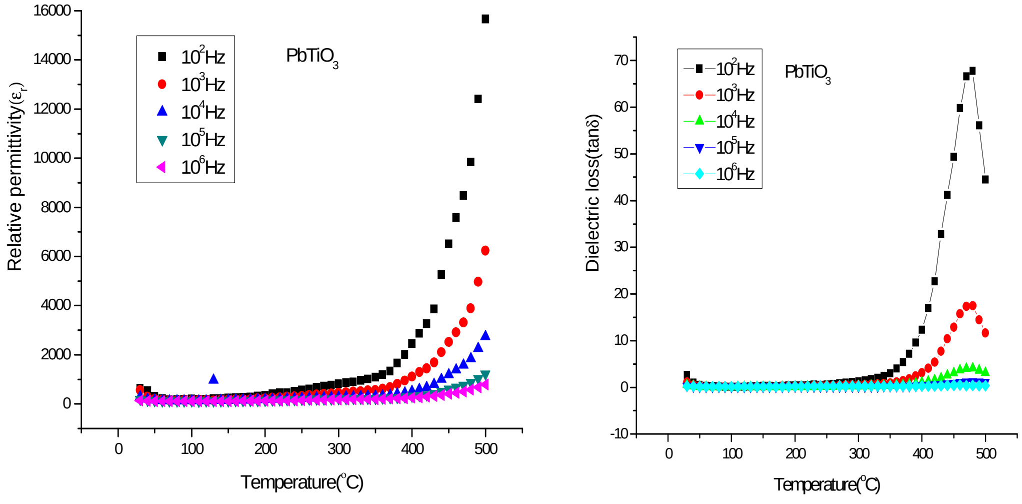

(a) (b)

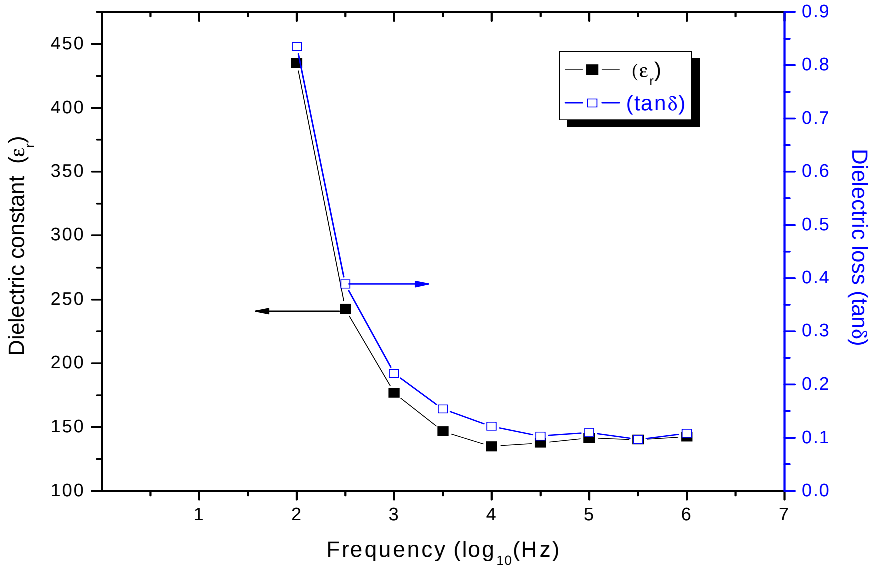

(c)

Fig.7 (a) Temperature-frequency dependence of relative permittivity (ε_r) (b) Temperature-frequency dependence of dielectric loss (tanδ) (c) variation of dielectric constant and loss factor with frequency of $PbTiO_3$ ceramic sample sintered at 1000°C

Fig. 7a shows the temperature variation of ε_r at different frequencies (100Hz–1 MHz) of PT samples. Values of ε_r at different frequencies increases with the increase in temperature. The increase in dielectric constant with increase in temperature takes place because polarization is an inherent property of ferroelectrics and the electron transfer increases due to thermally activated electrons. From these plots, it is clear that the dielectric constant slowly increases with increase in temperature up to 350°C due to its high resistivity, impurities and defects in the materials. Further increase in temperature increases the dielectric constant up to the transition temperature and decreases there after [25, 26]. The change in dielectric constant takes place due to exchange interaction between the electrons at transition temperature. The electron exchange in the ferroelectrics is due to local displacement of charges in the direction of applied electric field, which determines the polarization of the phases. In the present case, exchange of electron takes in titanium as $Ti^{4+} \rightarrow Ti^{3+}$. However, the value of dielectric constant is found to be enhanced. This enhancement in dielectric constant can be understood by possible formation of smaller crystallite size which in turn results as good grain connectivity and high density. Parameters like good grain connectivity and high density may produce easy transfer of electrons which forms electric dipoles. Considering a heterogeneous system with grains and grain boundaries possessing different conducting properties, the variation in dielectric constant can be viewed from a different perspective and transition temperature (T_c) was found to be around 493°C. In case of nano-particles, the number of grains and grain boundaries is large and hence a large dielectric constant is expected. So the observed enhancement in the dielectric constant in the nano-system can be directly associated with the presence of numerous nano-sized grains and interfaces. Therefore, the value of dielectric constant at transition temperature is found to be higher for the sample prepared by ceramic method. The ε_r at different frequencies increases with the increase in temperature and ε_r of any material, in general, is influenced by dipolar, electronic, ionic and interfacial polarizations [27-28]. Interfacial polarization increases due to the creation of crystal defects and dipolar polarization decreases due to the increase in randomness of the dipoles with temperature. However, the temperature effect on ionic and electronic polarizations is very small [29]. The increase in ε_r with temperature suggests the increase in interfacial polarization. At 40°C, values of ε_r at 100Hz was found to be 550.6256, which increases drastically to 15657.45 at the transition temperature. Value of T_c 493ºC is in accordance with earlier reports on PT system [29].

Fig.7 (b) shows that the temperature variation of tanδ at different frequencies (100Hz to 1MHz) of $PbTiO_3$ ceramic sample. The values of tanδ at different frequencies increases with the increase in temperature and above transition temperature it falls sharpely.At around 40ºC the loss factor was 1.022668 at frequency 100Hz which increases suddenly to 67.6954 at transition temperature and after that it falls to 44.5194.

Fig.7(c) shows the frequency dependence of ε_r and tanδ at room temperature of $PbTiO_3$ ceramic samples. At 30°C, values of ε_r and tanδ at 1MHz are found to be 435.004 and 0.8344. Initially, both ε_r and tanδ decreases with the increase in frequency, which is a normal behavior of dielectric/ferroelectric materials [30]. The fall in ε_r arises from the fact that polarization does not occur instantaneously with the application of the electric field, which is further due to the inertia of the dipoles and the delay in response towards the impressed alternating electric field leads to dielectric loss and decline in ε_r. At low frequencies, all types of polarization contributes and as the frequency is increased, polarizations with large relaxation times cease to respond and hence the decrease in ε_r [31-34]. At lower frequencies ε_r is maximum because the contributions from the space charge polarization is large. The space charge polarization arises by the accumulation of charges mainly due to vacancies of lead and oxygen at the grain boundaries and at the electrode interface. At higher frequencies, contributions from the polarizations having high relaxation time ceases resulting in the decrease in ε_r [35]. Among the tree types of polarizability which involves electron is fast process and so the electronic polarizability exists up to very high frequency ac fields, even upto UV range. The ionic and the dipolar polarizabilities which involve ions and dipoles is the slower process due to the inertia of ions and the molecular dipoles. The dipolar polarizability which is due to the orientation of dipoles is the slowest process. The dipoles can not respond beyond microwave frequency. Above microwave frequency, the contribution to the total polarizability is only from ionic and electronic process. The ionic contribution exists up to infrared frequencies. Beyond infrared, the displacement of ions cannot respond fast enough due to inertia of ions. So the contribution beyond infrared is only due to electronic polarizability. The same type of frequency-dependent dielectric behaviour is found in many other ferroelectric ceramic systems [36-40].

Conclusion

We have prepared a single phase $PbTiO_3$ compound by following the solid state route. All the observed peaks could be indexed to *P4mm* space group with tetragonal symmetry. From Rietveld analysis the unit cell parameters are found to be a=b=3.8987(0.0008)Å and c=4.1380(0.0009)Å. The axial ratio c/a is found to be 1.0614 which is less then that of reported value 1.0630. Hence, we could prepare with low axial ratio compound by following solid state route. The average axial and in plane bond lengths are found to be 1.8865Å and 2.0026Å respectively. SEM and EDS measurement shows that the material is uniform and the composition at different places are found to be identical. The c/a ratio does not differ between samples sintered at different temperatures and hence does not appear to be critical in influencing micro cracking. Changes in the crystallite size and the occurrence of Pb vacancies during sintering of PT powders between 600ºC and 1000ºC may be used to account for the Pb loss characteristics of PT and related ceramics. Dielectric constant was found to be 15657.45 and the Value of Tc was found to be ~493ºC. The proposed reaction and preparation method turned out to be useful for synthesis of PbTiO3 ferroelectric with superior properties, smaller grain size and low temperature sintering (Microwave sintering) which avoids lead loss suggesting its suitability for other lead-based ferroelectrics such as PZT, PLZT, PLZFT, PLZMT, PCT, PLT, PLTA, PBT, etc., which are of current interesting technologically important ceramic materials.

Acknowledgements

All the experimental works have been carried out using the facilities available at the Centre for Nanotechnology, IIT Guwahati. Authors are thankful to the Head, Centre for Nanotechnology, IIT Guwahati for extending the facilities to carry out the experimental work. Authors are also thankful to the Head, Ceramic Engineering Department, NIT, Rourkela for electrical measurements.

References

[1] R. Ramesh, D.G. Schlom, *Science* 296 **(2002)** 1975.
[2] D.D. Fong, G.B. Stephenson, S.K. Streiffer, J.A. Eastman, O. Auciello, P.H. Fuoss, et al., *Science* 304 **(2004)** 1650.
[3] A.G. Zembilgotov, N.A. Pertsev, H. Kohlstedt, R.Waser, *J. Appl. Phys*. 91 **(2002)** 2247.
[4] Q. Jiang, X.F. Cui, M. Zhao, *Appl. Phys. A-Mater* 78 **(2004)** 703.
[5] H.X. Fu, L. Bellaiche, *Phys. Rev. Lett*. 91 **(2003)** 257601.
[6] K. Ishikawa, K. Yoshikawa, N. Okada, *Phys. Rev. B*, 37 **(1988)** 5852.
[7] X.Y. Lang, Q. Jiang, *J. Nanopart. Res. 9* **(2007)** 595.
[8] S. Zhang, H. Li and M. Li, *Materials letters*, 62 **(2008)** 2438.
[9] S. Kim, M.-C. Jun, S.-C. Hwang, *J. Am. Ceram. Soc*. 82 **(1999)** 289.
[10] P. L¨obmann, W. Glaubitt, *J. Am. Ceram. Soc*. 80 **(1997)** 2658.
[11] S. Iakovlev, C.-H. Solterbeck, M. Es-Souni, V. Zaporojtchenko, *Thin Solid Films* 446 **(2004)** 50.
[12] F. Jona and G. Shirane, *Ferroelectric crystals*, Dover publications, Inc., New York, **1993.**
[13] P.P. Neves, A. C. Doriguetto, V. R. Mastelaro, L. P. Lopes, Y. P. Mascarenhas, A. Michalowicz, J. A. Eiras. *J Phys Chem B* 108 **(2004)** 14840.
[14] R. Tickoo, R. P.Tandon, V. K. Hans, K. K. Bamzai, P. N. Kotru. *Mat. Sci Eng B* 94**(2002)** 1
[15] K. Wójcik, *Ferroelectrics* 99 **(1989**)5.
[16] R. A. Young, *"The Rietveld Method"* International Union of Crystallography, (New York, Oxford University Press **1996**).
[17] S. Ananta, N.W. Thomas, *J. Eur. Ceram. Soc.* 19 **(1999)** 2917–2930.
[18] L.S. Hong, C.C. Wei, *Mater. Lett.* 46 **(2000)** 149–153.

[19] S. Kim, M. Jun, S. Hwang, *J. Am. Ceram. Soc.* 82 **(1999)** 289–296.
[20] K. Katayama, M. Abe, T. Akiba, H. Yanagida, *J. Eur. Ceram. Soc.* 5 **(1989)** 183–191.
[21] C.J. Howard, B.A. Hunter, Acomputer program for Rietveld analysis of X-ray and neutron diffraction patterns, *ANSTO Lucas Heights Research Laboratories*, **1997.**
[22] K. Kakegawa, S. Saori, N. Uekawa, *J. Eur. Ceramic Soc.* 26 **(2006)** 613.
[23] A. Pel´aiz-Barranco, Y. Gonz´alez-Abreu, *Solid State Communications* **(2009),** doi: 10.1016 / j.ssc.2009.08.012
[24] S. Chopra, S. Sharma, T. C. Goel, R. G. Mendiratta, *Appl. Sur. Sci.*, 230 **(2004)** 207.
[25] Introduction to Solid State Physics by Charles Kittel, Wiley, New York, **(1995).**
[26] J. Mal and R.N.P. Choudhary, *Phase Transitions* 62 **(1997)** 19.
[27] N. K. Mishra, R. Sati, R.N.P. Chaoudhary, *Mater. Lett.* 24 **(1995)** 313.
[28] A. K. Singh, T. C. Goel, R. G. Mendiratta, O. P. Thakur and C.Prakash: *J. Appl. Phys.* 91 **(2002)** 6626.
[29] S. Chopra, S. Sharma, T.C. Goel and R.G. Mendiratta, *Materials Chemistry and Physics* 91 **(2005)** 161–165.
[30] E. Sato, Y. Huang, M. Kosec, A. Bell, N. Setter, *Appl. Phys. Lett***.** 65 **(1994)** 2678.
[31] K.K. Patankar, S.L. Kadam, V.L. Mathe, C.M. Kanamadi, V.P. Kothavale, B.K. Chougule, *Br. Ceram. Trans.* 19 **(2003)** 102.
[32] S.L. Kadam, K.K. Patankar, V.L. Mathe, M.B. Kothale, R.B. Kale, B.K. Chougule, *J. Electro ceram.* 9 **(2003)** 193.
[33] D. Alder, Feinleib, *J. Phys. Rev. B* 2 **(1970)** 3112.
[34] B.D. Cullity, Elements of X-Ray Diffraction, 2nd ed., Addison-Wesley Publishing Company, Inc., United States of America, **1978**, p. 89.
[35] H. Klug, L. Alexander, X-ray Diffraction Procedures for Polycrystalline and Amorphous Materials, 2nd ed., Wiley, New York, **1974.**
[36] A. Rujiwatra, N. Thammajak, T. Sarakonsri, R. Wongmaneerung, S. Ananta, *J. Crystal Growth* 289 **(2006)** 224–230.
[37] H. Beltran, N. Maso, E. Cordoncillo, A.R. West, *J. Electroceram.* 18 **(2007),** 277–282.
[38] S. Jiansirisomboon, A. Watcharapasorn, *Curr. Appl. Phys.* 8 **(2008)** 48–52.
[39] R. Gadow, F. Kern, A. Killinger, *Mater. Sci. Eng. B* 148 **(2008)** 58–64.
[40] A.J. Moulson, J.M. Herbert, Electroceramics, 2nd ed., Wiley, Chichester, **2003.**